ACS APPLIED MATERIALS & INTERFACES

Research Article

www.acsami.org

Accelerated Formation of Metal Oxide Thin Film at 200 °C Using Oxygen Supplied by a Nitric Acid Additive and Residual Organic Suction Vacuum Annealing for Thin-Film Transistor Applications

Woong Hee Jeong, Dong Lim Kim, and Hyun Jae Kim*

School of Electrical and Electronic Engineering, Yonsei University 50 Yonsei-ro, Seodaemun-gu, Seoul 120-749, Republic of Korea

Supporting Information

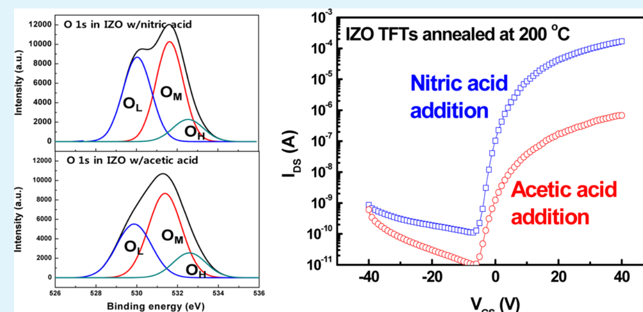

ABSTRACT: Oxide semiconductors have gradually replaced amorphous and polycrystalline silicon for thin-film transistor (TFT) because of their high mobility and large-area uniformity. Especially, the oxide semiconductors have also achieved the low-cost manufacturing using a solution process. However, because the solution-processed oxide semiconductors require a high thermal energy to form the oxide thin film, the additional solution synthesis and annealing process are needed for low-temperature solution process. Because the conventional solution-processed oxide thin films have low oxidation level and high residual organic concentration at low annealing temperature, we propose the novel solution process that includes the nitric acid additive and the vacuum ambient annealing as an oxidizing agent and a residual organic suction, respectively. Therefore, we have successfully developed the simple oxide solution process and the soluble InZnO TFT with high field-effect mobility of 3.38 $cm^2/(V\ s)$ at 200 °C.

KEYWORDS: *low-temperature process, nitric acid, vacuum annealing, oxide thin-film transistor, and flexible electronics*

INTRODUCTION

Recently, various approaches for active semiconductor layer in the thin-film transistor (TFT) technology applications have been conducted using polycrystalline silicon, organic semiconductor, and oxide semiconductor.[1−3] In particular, oxide semiconductor, deposited by physical or chemical deposition, is widely believed to be an attractive material because of their electrical characteristics, transparency, and large deposition area.[4−7] Solution-processed oxide semiconductor film has also attracted much attention recently because of low processing cost, direct printing applications, and availability of various oxide compositions,[8−11] suggesting the use of oxide films for large-area, flexible electronics in next-generation applications.

The thermal annealing process used in the formation of a solution-processed oxide film involves several key steps: the decomposition of the metal precursor, evaporation of the solvent and residual organics, formation of the oxide film, and enhancement of the film density.

Therefore, thermal annealing above 450 °C is required to produce solution-processed oxide films with high purity and density.[12−14] Studies have shown that as the annealing temperature decreases below 300 °C, the TFT suffers from a low field-effect mobility (μ_{FE}) and a large hysteresis; this was attributed to poor film quality resulting from atomic disorder and residual organics.[15,16] For those reasons, it has been difficult to produce high-quality metal-oxide thin films at lower temperatures using conventional oxide solution processes that require metal salt precursors and organic solvents.

Several low-temperature solution-processing methods have been used to produce oxide TFTs,[15−19] involving various combinations of modulated alkoxide[15] and hydroxide[19] precursors, acetyl acetone and urea catalysts,[16] and annealing conditions (using steam,[15] ozone,[17] pressure,[18] and microwaves[19]); all of these approaches involve rapid metal-oxide formation and organic annihilation at low temperature. Here, we proposed a novel volatile oxide solution for low-temperature TFT fabrication at 200 °C. The solution synthesized was based on the volatile decomposition of a nitrate precursor[20,21] and an oxygen-supplying nitric acid additive. The nitrate precursor easily decomposed into metal cations and nitrate anions at low temperature.[20] The nitric acid additive supplied the oxygen to the IZO solution and enhanced the hydrolysis reaction of the ionized metals. Thermal annealing under vacuum ambient induced evaporation of the residual organic material and enhanced the film quality. On the basis of the volatile oxide solution and vacuum annealing, we fabricated an InZnO (IZO) TFT with a high μ_{FE} of 3.38 $cm^2/(V\ s)$ and low hysteresis at 200 °C.

Received: June 12, 2013
Accepted: August 20, 2013
Published: August 20, 2013

ACS Publications © 2013 American Chemical Society

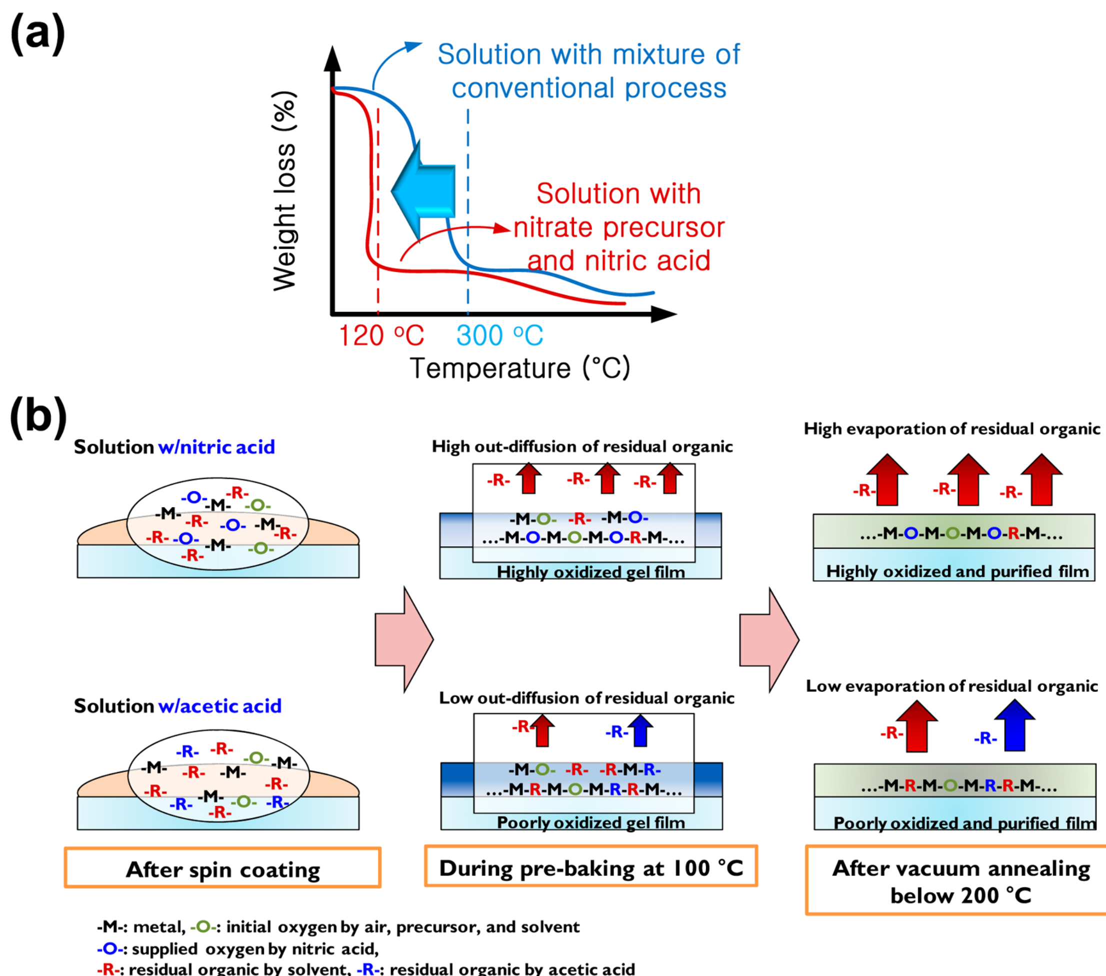

Figure 1. Illustration for roles of nitric acid and vacuum annealing for the low-temperature oxide thin-film fabrication: (a) TG-DTA schematic of the IZO (In/Zn = 5) solution at different pH levels (conventional process using several metal-salt precursors and additives of acetic acid/monoethanolamine, pH 7; new process using the nitrate precursor and nitric acid additive, pH 1), (b) chemical reaction with processing flow.

EXPERIMENTAL DETAILS

Preparation of IZO Solutions. The sol−gel method was used to prepare the IZO solutions; indium nitrate and zinc nitrate were used as the precursors. The solvent for the IZO solutions was 2-methoxyethanol (2ME). The molar ratio of In to Zn varied from 1:1 to 9:1 and pure In_2O_3; the molar concentration of the IZO solutions was held constant at 0.3 M. Additives of nitric acid or acetic acid were added to the mixture following dissolution using 2ME. The IZO solutions were kept at 60 °C and stirred at 340 rpm for 1 h. The solutions were filtered through a 0.2 μm syringe filter. The IZO solution with nitric acid was stable during 10 months after the IZO solution fabrication.

IZO TFT Fabrication. The IZO TFTs discussed in this study consisted of a bottom-gate and inverted staggered TFT structure. A 200-nm-thick MoW gate electrode was attached to a SiO_2/glass substrate using sputtering deposition. The gate insulator was a 120-nm-thick SiO_2 layer that was deposited on the patterned gate electrode by plasma-enhanced chemical vapor deposition. The IZO solution was spin-coated at 3000 rpm for 30 s. Then, the spin-coated IZO films were pre- and postannealed at 100 and 200 °C for 10 min and 3 h in air and vacuum ambient, respectively. The thickness of the IZO film was ∼27 nm after the postannealing process. The source and drain electrodes consisted of 100 nm thick Al, which was evaporated onto the IZO film using sputtering deposition. The width/length (W/L) ratio of 1000/100 μm (10) was held constant for the IZO TFTs. Polymethyl methacrylate (PMMA) was used as the passivation layer in the IZO TFTs. The PMMA was spin-coated on IZO TFT at 1000 rpm for 30 s and the IZO TFTs were annealed at 100 °C for 30 min.

Analyses of IZO Films and TFTs. X-ray photoelectron spectroscopy (XPS) (XPS, ESCALAB 220I XL, VG Scientific) was conducted at 100 °C to examine the chemical characteristics of the IZO films with respect to the additives, nitric acid and acetic acid. To detemine the concentration of residual organics in the IZO films, we determined the concentration depth profiles of carbon and hydrogen in the IZO films at 200 °C by secondary ion mass spectroscopy (TOF-SIMS, TOF-SIMS-5, ION-TOF) with respect to the additives. The density, thickness, and roughness of the nitric acid-IZO films at 200 °C were examined using X-ray reflectivity (XRR, RINT-TTR-MA, Rigaku) analysis. The electrical characteristics of the IZO TFT with respect to the additives and the In:Zn ratio were determined by an Agilent 4156C semiconductor analyzer in the dark at room temperature.

RESULTS AND DISCUSSION

Figure 1a shows the scheme of thermogravimetric analysis (TGA) of the different oxide solutions as a function of precursor and additive. During solution-processing of the oxide film, the evaporation of the solvent, the decomposition of the precursor, and the oxidation of decomposed metal cations were controlled by the pH, the type of precursor, and the concentration of residual organic material. It should be noted that these reactions (evaporation, decomposition, and oxidation) occurred simultaneously. The decomposition temperatures of the oxide solution decreased at lower pH, as shown in Figure S1a in the Supporting Information. Nitric acid

dx.doi.org/10.1021/am4022818 | ACS Appl. Mater. Interfaces 2013, 5, 9051−9056

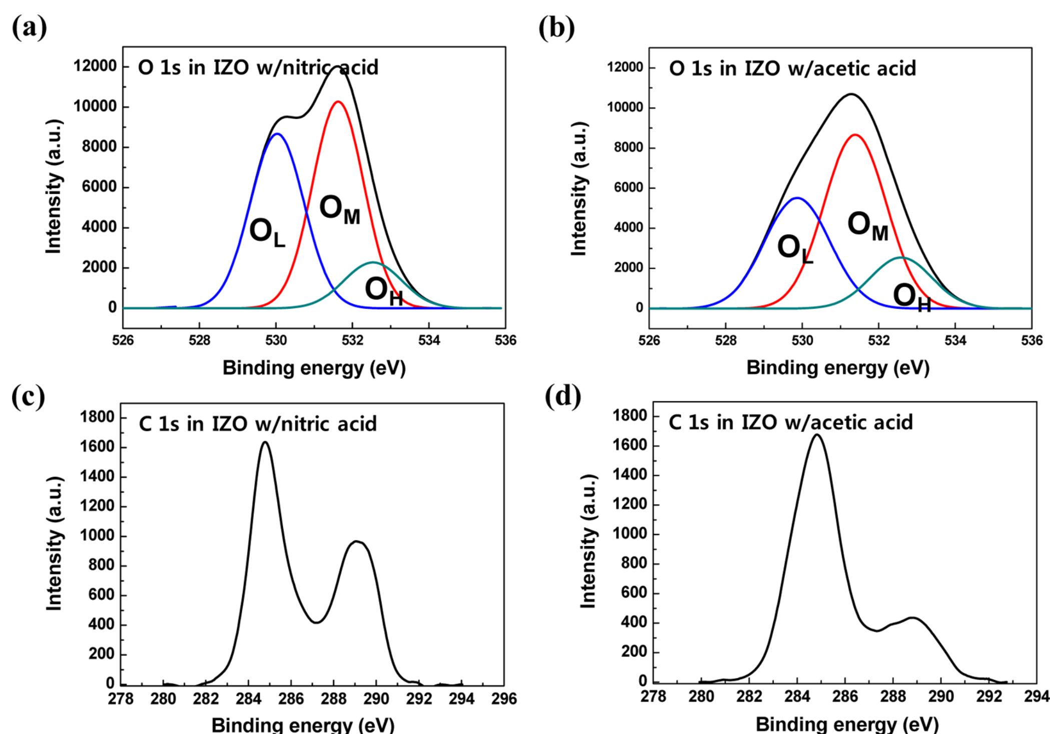

Figure 2. XPS spectra of O 1s and C 1s peaks for the IZO at 100 °C with respect to the additives: (a, c) nitric acid; (b, d) acetic acid, respectively.

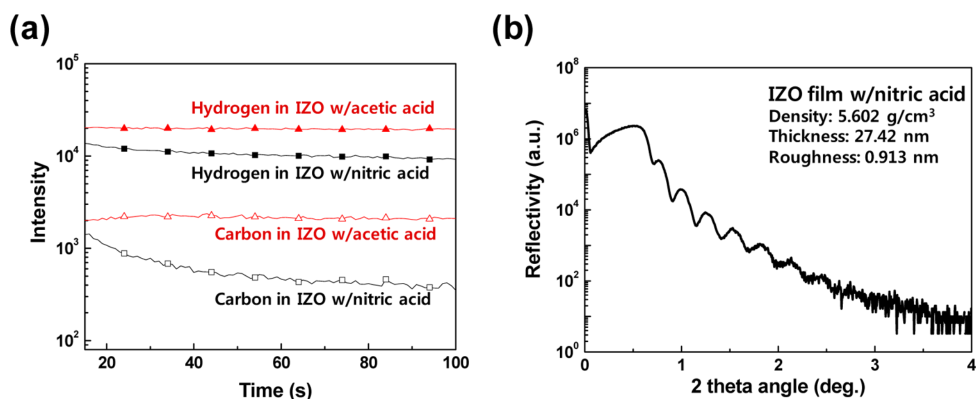

Figure 3. (a) SIMS of the IZO thin films with respect to the additives and (b) XRR analyses of the IZO thin film with nitric acid additive.

has a low pH of 1 and a low boiling point of 82 °C. Thus, the decomposition reaction of IZO with nitric acid occurred at a low temperature of ∼120 °C. Additionally, the nitric acid enhanced the solubility of the nitrate precursor in the organic solvent and maintained the stability of the oxide solution. However, nitric acid does not induce combustion because of its small exothermic peak near 120 °C (see the Supporting Information, Figure S1b).[16] Other research groups have reported from TGA that the nitrate precursor had the steepest weight loss because of its decomposition at lower temperatures.[22] The nitrate precursor can decompose volatilely into metal cations and salt anions. The IZO film fabricated by a nitrate precursor has a low concentration of residual organics.[20] Consequently, the IZO solution prepared by nitric acid and a nitrate precursor exhibited low-temperature evaporation and decomposition and produced high-quality IZO films compared to the other conventional solutions.

Additional oxygen was generated during nitrogen dioxide formation in nitric acid, as indicated by the chemical reaction with overall flow process shown in Figure 1b. The nitric acid not only enhanced the decomposition of the IZO solution and the solubility of the nitrate precursor but was also a strong oxidizing agent because of its large positive reduction potential. Nitric acid reacts violently, as a general rule, and additional oxygen is generated during nitrogen dioxide formation. The additional oxygen anions can promote the hydrolysis reaction of a metal cations.

To determine the effect of nitric acid as an oxidizing agent, we analyzed X-ray photoelectron spectroscopy (XPS) spectra of the IZO film with respect to the nitrate acid and acetic acid additives. The IZO solutions were prepared using the same In and Zn nitrate precursors in an In:Zn ratio of 5:1. The prebaked IZO films were annealed at 100 °C for 10 min in ambient air. Panels a and b in Figure 2 compare the O 1s peaks of nitric acid and acetic acid added to the IZO solution, respectively. In general, the Gaussian-fitted subpeaks in the O 1s peak are composed of O_L, O_M, and O_H located at 530.1, 531.6, and 533.5 eV, which denote metal−oxygen bonding,

 dx.doi.org/10.1021/am4022818 | ACS Appl. Mater. Interfaces 2013, 5, 9051−9056

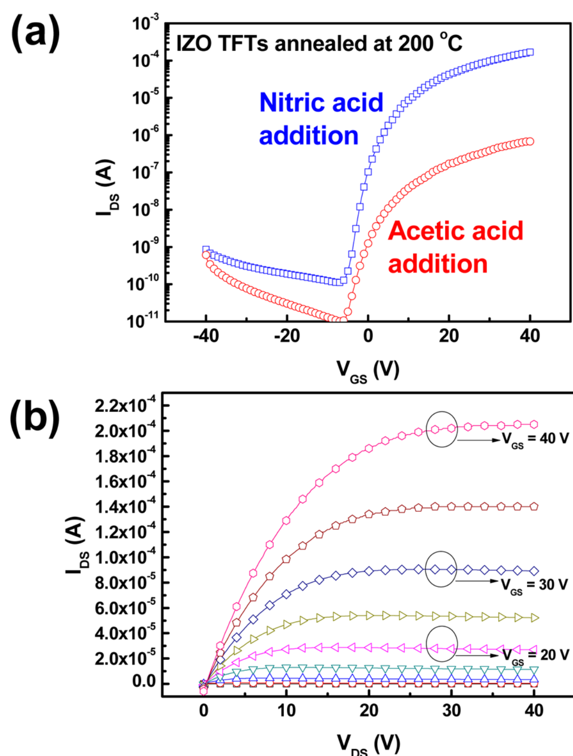

Figure 4. (a) Comparison of IZO TFTs with respect to the additives and (b) output characteristics of IZO TFT with a nitric acid additive.

Table 1. Transfer Parameters of IZO TFTs with Various Composition Ratios at 200 °C Vacuum Annealing

material	composition ratio (In:Zn)	μFE (cm^2/(V s))	ion/off	V_{th} (V)	S.S. (V/decade)
IZO	1:1	0.003	7.65 × 105	19.56	0.82
	3:1	0.571	5.95 × 105	14.32	1.42
	5:1	3.378	1.45 × 106	13.73	1.55
	7:1	4.442	2.29 × 105	2.34	1.50
	9:1	0.507	3.96 × 105	8.55	1.64
In_2O_3		0.041	6.44 × 104	13.91	2.83

oxygen vacancy in the oxide, and an loosely bond oxygen on the surface, respectively.[18,23] The O 1s peak indicated obviously that $O_L/(O_L + O_M + O_H)$ value of IZO with nitric acid was 0.415 larger than that of the acetic acid-IZO film (0.342). Because nitric acid acts as a strong oxidizing agent at prebaking stage shown in center of Figure 1b, the produced oxygen anions would increase the probability of metal cation oxidation through a hydrolysis reaction. During the annealing process, in addition to the oxygen generated from nitrate anions and ambient air, decomposed In and Zn cations combined with the oxygen supplied by the nitric acid; this was more likely to occur with the nitric acid additive than with acetic acid. Eventually, the larger area of the O_L peak suggested that nitric acid supply oxygen to the oxide solution. The smaller area of the O_L peak in the acetic acid-IZO was attributed to low oxygen binding due to the strong C−O bond in the acetic acid.[12] The O_M peak of the O 1s peak would reveal not only oxygen defects, but also the structural incompletion of the oxide film. The O_H peak of the O 1s peak would also corresponded to surface dangling bonds and morphology. The larger area of the O_M and O_H peaks in acetic acid-IZO reflected that it would have poor film quality at low temperature. Therefore, these results indicate that the formation of an oxide film using an acetic acid additive would require a higher thermal energy than that using a nitric acid additive.

Figure 2 (c) and (d) show the C 1s peaks in the IZO films, which were attributed to the additives. In contrast to the oxygen trends, the C 1s peak of IZO with nitric acid had somewhat higher intensity than that with the acetic acid additive. This suggested that the weakly bonded carbon-related residual organics diffused outward toward the surface during prebaking stage using a hot plate (as shown in Figure 1b). Figure S2 in the Supporting Information shows the In $3d_{5/2}$ and Zn $2p_{3/2}$ peaks of the two IZO films with nitric and acetic acid additives at 444.6 and 1021.7 eV, respectively. It also indicated that the IZO solutions with low pH could form the IZO lattice at 100 °C.

For the low-temperature process, high-purity IZO formation which had a low concentration of residual organic was a concern. With the exception of the nitrate precursor and nitric acid, the coated oxide film would contain organic residue due to the organic solvent and additives.[12,20] Thus, it is still difficult to attain the high-purity oxide film and the annealing process with another treatment is needed at low temperature. Vacuum annealing could be an effective option for the physical removing the residual organics to enhance not only the purity, but also the density of the solution-processed IZO films except through the thermal energy. To evaporate the residual organic at low temperature, the annealing process was conducted under vacuum ambient, as shown in the right of Figure 1b. Figure 3a shows the concentration depth profiles from secondary ion mass spectroscopy (SIMS) analysis for carbon and hydrogen in the IZO films (In:Zn = 5:1) with respect to the additives, annealed at 200 °C under vacuum ambient. Because the buried carbon and hydrogen could disturb the lattice formation of the IZO films, lowering the impurity concentration induced bonding between the metal and oxygen, and increased the film density.

We found that as the sputtering time increased (from surface to bulk of IZO films), the impurity concentration of the IZO by nitric acid was lower than those by acetic acid. Eventually, even in the same vacuum annealing condition, the impurities in the oxide film could be determined by additive. Although the nitrate precursor was ionized at lower temperature, the ionized metal could easily combine not only with the oxygen from the nitric acid and the air, but also with the residual organic related to carbon and hydrogen in the additive−solvent mixture. Consequently, it was important to suppress the bonding between the metal and the residual organic material, and to reduce the organic impurities in the IZO lattice. However, it should be noted that the IZO with acetic acid had a higher concentration of residual organics due to the intermediated metal-residual organic bonding.

As aforementioned, because the metal cation was bonded easily to the supplied oxygen anion by nitric acid, the coherence of the residual organic in IZO lattice became weak. Therefore, the weakly bonded or existed organics were easily removed by the low-temperature vacuum annealing process. Furthermore, following vacuum annealing, the IZO film density with a nitric acid was further increased by the structural relaxation that occurred under the annihilation of the weakly bonded or existed residual organics. An increase in the solution-processed oxide film density was promoted by high annealing temperatures and low residual organic concentrations in the oxide film.[24] Figure 3b shows the X-ray reflectivity (XRR) of the IZO

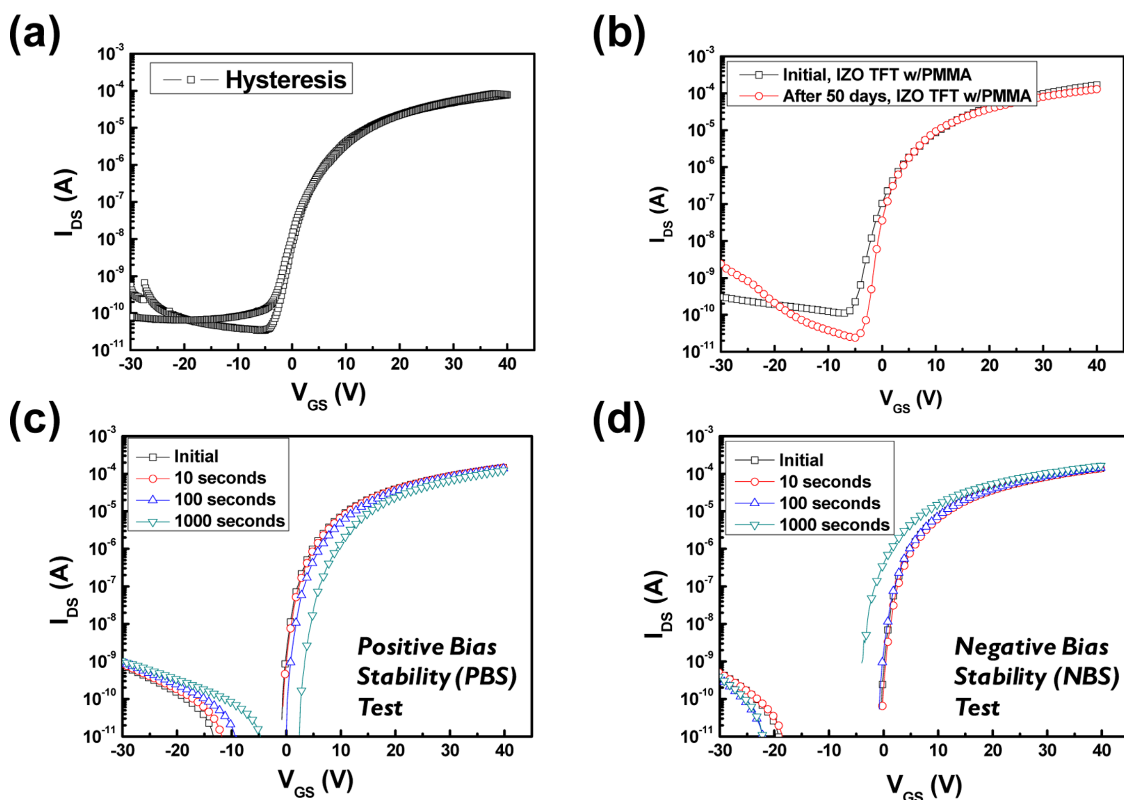

Figure 5. Various stability tests of IZO TFT with In:Zn = 5:1: (a) hysteresis, (b) aging test (with PMMA passivation layer), and bias stress applied with a (c) positive and (d) negative bias.

with the nitric acid additive; the results indicate a density of 5.602 g cm^{-3}, a thickness of 27.42 nm, and a surface roughness of 0.913 nm for the IZO film. Although the density of the solution-processed IZO was lower than that (5.9 g/cm^3) of amorphous indium−gallium−zinc-oxide by the sputtering method,[25] it was much higher than that (4.334 g/cm^3) of the solution-processed IZO annealed at 220 °C in ambient air.[18]

We then compared the electrical properties of IZO TFTs produced using IZO solutions with different additives; the IZO TFTs were vacuum annealed at 200 °C for 3 h. The electrical characteristics of the different IZO TFTs are shown in Figure 4a. The IZO TFT with an acetic acid additive exhibited poor electrical characteristics, such as a μ_{FE} of 0.02 cm^2/(V s), an on/off current ratio ($I_{on/off}$) of 6.77 × 10^4, a threshold voltage (V_{th}) of 15.74 V, and a subthreshold swing (S.S.) of 2.34 V/decade. In contrast, the electrical characteristics of the IZO TFT with a nitric acid additive were significantly better, exhibiting a μ_{FE} of 3.38 cm^2/(V s), an $I_{on/off}$ of 1.45 × 10^6, a V_{th} of 13.73 V, and a S.S. of 1.55 V/decade. From this comparison, under identical preparation conditions (i.e., using the same precursor, solvent, and annealing procedure), the proper choice of oxidizing agent additive was crucial to the electrical characteristics of the IZO TFT at low temperature. The improved electrical characteristics of the IZO TFT were due to the low residual organic concentration and the high density of the IZO by a nitric acid addition. Current crowding and kink effect were not evident in the TFT output curves shown in the Figure 4b. The IZO TFT exhibited good linear/saturation behavior, and the corresponding regions of the output curves were well-separated.

To determine the effect of concentration of nitric acid, we also fabricated the IZO TFTs with respect to different concentrations of nitric acid over solvent. Increased nitric acid concentration degraded the electrical characteristics of IZO TFTs, as shown in the Supporting Information, Figure S3; this would be attributed to the difference in oxidation level of the IZO as the nitric acid concentration increased.

We varied the In:Zn ratio from 1:1 to 9:1 and pure In_2O_3 to determine the effect of In concentration on the electrical properties of the IZO TFTs. The results are shown in the Table 1. As the In content increased, the conductivity of the IZO also increased. The highest conductivity corresponded to the IZO with an In:Zn ratio of 7:1; however, the conductivity decreased for In:Zn ratio of 9:1 and pure In_2O_3. These results revealed that the generation of the oxygen vacancies in the In-rich region decreased as the In:Zn ratio approached pure In_2O_3.[15] The electrical characteristics of the IZO TFTs followed the trends in the conductivity of the IZO. The IZO TFT that was optimized with respect to μ_{FE}, V_{th}, and $I_{on/off}$ had an In:Zn ratio of 5:1.

Besides μ_{FE}, the electrical stability of a solution-processed oxide TFT at low temperature can be a significant issue for flexible electronics. Figure 5 shows the stability evaluations of the IZO TFT with a nitric acid additive in terms of hysteresis, aging, and bias stress test results. Hysteresis phenomenon was not observed in the transfer curve, as shown in the Figure 5a. After 10 days without passivation in ambient air, the transfer characteristics of the nitric acid IZO TFT deteriorated; the μ_{FE} decreased and the V_{th} increased. These results were attributed to oxygen absorption from an ambient air, which lowered the conductivity (as shown in the Supporting Information, Figure S4). The IZO TFT with polymethyl methacrylate (PMMA) passivation exhibited a slight change in its electrical characteristics after 50 days of aging (Figure 5b); the off-current and S.S. decreased slightly because the organic PMMA layer allowed oxygen to penetrate the IZO bulk. Positive and negative bias

dx.doi.org/10.1021/am4022818 | ACS Appl. Mater. Interfaces 2013, 5, 9051−9056

stress tests (PBS and NBS tests, respectively) were also carried out under a gate to source voltage,V_{GS}, of +20 and −20 V, respectively, with a drain to source voltage, V_{DS}, of 10 V for 1000 s. Panels c and d in Figure 5 show V_{th} shifts of +3.2 and −3.6 V in the PBS and NBS tests, respectively, for the applied gate polarity. The change in the S.S. was negligible during the bias stability test; there was no indication of trap state creation in the interface between the gate insulator and semiconductor or in the IZO bulk.[26] However, the drain current was interrupted by the simultaneous trapping and release of carriers in the trap state during the V_{GS} sweep. Finally, there were uniform transfer characteristics in a substrate with a square 30 mm on a substrate .

CONCLUSIONS

In summary, using a novel volatile solution and vacuum annealing, a high-purity, robust IZO TFT was produced at low temperature. This electrically stable IZO TFT was comparable to other solution-processed oxide TFTs produced at high temperatures.[27,28] The decomposed metal cations from the nitrate precursor were oxidized effectively due to the sufficient oxygen supply from a nitric acid additive. Formation of the IZO lattice by oxygen supplied from the nitric acid suppressed bonding between intermediate metal and organics. Because the residual organic material in the IZO film was weakly bonded or existed, it evaporated easily from IZO film under vacuum annealing at 200 °C. Vacuum annealing could also increase the density of IZO film by structural relaxation. The resulting IZO film had a high density and purity, and the IZO TFT produced using these films exhibited high electrical characteristics and device stability for flexible electronics.

ASSOCIATED CONTENT

Supporting Information

Several results for chemical and electrical characteristics of IZO solutions, films, and TFT. This material is available free of charge via the Internet at http://pubs.acs.org/.

AUTHOR INFORMATION

Corresponding Author

*E-mail: hjk3@yonsei.ac.kr.

Notes

The authors declare no competing financial interest.

ACKNOWLEDGMENTS

This work was supported by the National Research Foundation of Korea (NRF) grant funded by the Korean Ministry of Education, Science and Technology (MEST) [no. 2011-0028819] and was also supported by the Industrial Strategic Technology Development Program (10041808,Synthesis of Oxide Semiconductor and Insulator Ink Materials and Process Development for Printed Backplane of Flexible Displays Processed Below 150 °C) funded by the Ministry of Knowledge Economy (MKE, Korea).

REFERENCES

(1) Im, J. S.; Kim, H. J.; Thomson, M. O. *Appl. Phys. Lett.* **1993**, *63*, 1969−1971.
(2) Fukuda, K.; Sekitani, T.; Zschieschang, U.; Klauk, H.; Kuribara, K.; Yokota, T.; Sugino, T.; Asaka, K.; Ikeda, M.; Kuwabara, H.; Yamamoto, T.; Takimiya, K.; Fukushima, T.; Aida, T.; Takamiya, M.; Sakurai, T.; Someya, T. *Adv. Funct. Mater.* **2011**, *21*, 4019−4027.
(3) Nomura, K.; Ohta, H.; Takagi, A.; Kamiya, T.; Hirano, M.; Hosono, H. *Nature* **2004**, *432*, 488−492.
(4) Fortunato, E. M. C.; Barquinha, P. M. C.; Pimentel, A. C. M. B. G.; Gonçalves, A. M. F.; Marques, A. J. S.; Pereira, L. M. N.; Martins, R. F. P. *Adv. Mater.* **2005**, *17*, 590−594.
(5) Nomura, K.; Ohta, H.; Ueda, K.; Kamiya, T.; Hirano, M.; Hosono, H. *Science* **2003**, *300*, 1269−1272.
(6) Jeong, J. K.; Jeong, J. H.; Yang, H. W.; Park, J.-S.; Mo, Y.-G.; Kim, H. D. *Appl. Phys. Lett.* **2007**, *91*, 113505−1−113505−3.
(7) Suresh, A.; Wellenius, P.; Dhawan, A.; Muth, J. *Appl. Phys. Lett.* **2007**, *90*, 123512−1−123512−3.
(8) Norris, B. J.; Anderson, J.; Wager, J. F.; Keszler, D. A. *J. Phys. D: Appl. Phys.* **2003**, *36*, L105−L107.
(9) Ong, B. S.; Li, C.; Li, Y.; Wu, Y.; Loutfy, R. *J. Am. Chem. Soc.* **2007**, *129*, 2750−2751.
(10) Lee, D.-H.; Chang, Y.-J.; Herman, G. S.; Chang, C.-H. *Adv. Mater.* **2007**, *19*, 843−847.
(11) Kim, H. S.; Byrne, P. D.; Facchetti, A.; Marks, T. J. *J. Am. Chem. Soc.* **2008**, *130*, 12580−12581.
(12) Kim, G. H.; Shin, H. S.; Ahn, B. D.; Kim, K. H.; Park, W. J.; Kim, H. J. *J. Electrochem. Soc.* **2009**, *156*, H7−H9.
(13) Seo, S.-J.; Choi, C. G.; Hwang, Y. H.; Bae, B.-S. *J. Phys. D: Appl. Phys.* **2009**, *42*, 035106−1−035106−5.
(14) Jeong, W. H.; Kim, G. H.; Shin, H. S.; Ahn, B. D.; Kim, H. J.; Ryu, M.-K.; Park, K.-B.; Seon, J.-B.; Lee, S.-Y. *Appl. Phys. Lett.* **2010**, *96*, 093503−1−093503−3.
(15) Banger, K. K.; Yamashita, Y.; Mori, K.; Peterson, R. L.; Leedham, T.; Rickard, J.; Sirringhaus, H. *Nat. Mater.* **2011**, *10*, 45−50.
(16) Kim, M.-G.; Kanatzidis, M. G.; Facchetti, A.; Marks, T. J. *Nat. Mater.* **2011**, *10*, 382−388.
(17) Han, S.-Y.; Herman, G. S.; Chang, C.-h. *J. Am. Chem. Soc.* **2011**, *133*, 5166−5169.
(18) Rim, Y. S.; Jeong, W. H.; Kim, D. L.; Lim, H. S.; Kim, K. M.; Kim, H. J. *J. Mater. Chem.* **2012**, *22*, 12491−12497.
(19) Jun, T.; Song, K.; Jeong, Y.; Woo, K.; Kim, D.; Bae, C.; Moon, J. *J. Mater. Chem.* **2011**, *21*, 1102−1108.
(20) Jeong, W. H.; Bae, J. H.; Kim, H. J. *IEEE Electron Device L.* **2012**, *33*, 68−70.
(21) Jeong, S.; Lee, J.-Y.; Lee, S. S.; Choi, Y.; Ryu, B.-H. *J. Phys. Chem. C* **2011**, *115*, 11773−11780.
(22) Prabhumirashi, L. S.; Khoje, J. K. *Thermochim. Acta* **2002**, *383*, 109−118.
(23) Fan, J. C. C.; Goodenough, J. B. *J. Appl. Phys.* **1977**, *48*, 3524−3531.
(24) Mitzi, D. B. *Solution Processing of inorganic Materials*; John Wiley & Sons: Hoboken, NJ, 2009; Chapter 2.
(25) Nomura, K.; Kamiya, T.; Ohta, H.; Uruga, T.; Hirano, M.; Hosono, H. *Phys. Rev. B* **2007**, *75*, 035212−1−035212−5.
(26) Jeong, J. K.; Yang, H. W.; Jeong, J. H.; Mo, Y.-G.; Kim, H. D. *Appl. Phys. Lett.* **2008**, *93*, 123508−1−123508−3.
(27) Park, K.-B.; Seon, J.-B.; Kim, G. H.; Yang, M.; Koo, B.; Kim, H. J.; Ryu, M.-K.; Lee, S.-Y. *IEEE Electron Device Lett.* **2010**, *31*, 311−313.
(28) Jung, Y.; Yang, W.; Koo, C. Y.; Song, K.; Moon, J. *J. Mater. Chem.* **2012**, *22*, 5390−5397.